Zoosyst. Evol. 102 (1) 2026, 97–105 | DOI 10.3897/zse.102.175615

An integrative description of a new interstitial species of *Boninia* (Platyhelminthes, Polycladida) from the South China Sea

Hai-Long Liu[1,2], Bing-Bing He[1], An-Tai Wang[1], Shuang-Fei Li[1], Yu Zhang[1]

1 *Shenzhen Key Laboratory of Marine Bioresource and Eco-environmental Science, Guangdong Engineering Research Center for Marine Algal Biotechnology, College of Life Sciences and Oceanography, Shenzhen University, Shenzhen, China*

2 *Key Laboratory of Optoelectronic Devices and Systems of Ministry of Education and Guangdong Province, College of Physics and Optoelectronic Engineering, Shenzhen University, Shenzhen, China*

https://zoobank.org/9E4B34A7-7712-431C-8CA1-6F579C7E981D

Corresponding author: Yu Zhang (biozy@szu.edu.cn)

Academic editor: Tom Artois ♦ **Received** 21 October 2025 ♦ **Accepted** 15 December 2025 ♦ **Published** 9 January 2026

Abstract

Some members of the genus *Boninia* are interstitial flatworms that have attracted research attention owing to their miniaturized body size and ecological significance. Here, we establish a new interstitial species of this genus, *Boninia corolla* **sp. nov.**, collected from a coarse-grained sandy beach in Huidong, China. The new species is characterized by (i) a narrow and slender body; (ii) 9–15 prostatoid organs with stylets arranged into a single girdle; and (iii) uterine canals connecting to the vagina immediately anterior to the entrance of Lang's vesicle. Results from both Bayesian Poisson Tree Process (bPTP) and Automatic Barcode Gap Discovery (ABGD) analyses support *B. corolla* **sp. nov.** as a distinct species. Molecular phylogenetic analyses based on four gene markers (18S, 28S, 16S, and COI) showed that the new species is nested within a clade composed of other *Boninia* species. We also calculated genetic distances between species based on the 28S, 16S, and COI markers and found that COI represents the most suitable DNA barcode for distinguishing species within the genus.

Key Words

Cotylea, DNA taxonomy, interstitial, marine flatworm, molecular phylogeny

Introduction

Marine interstitial meiofauna (also known as mesopsammon) are organisms that inhabit the interstitial spaces of marine sediments. They include representatives from most marine animal phyla, such as Coelenterata, Gnathostomulida, Kinorhyncha, Crustacea, Nemertea, Mollusca, etc. (Swedmark 1964; Higgins and Thiel 1988; Liu et al. 2022). Research attention on marine interstitial fauna began only in the early 20th century (Swedmark 1964), and current knowledge of their diversity is considered inadequate (Higgins and Thiel 1988; Worsaae and Kristensen 2005; Cerca et al. 2018). Polyclads are free-living flatworms (Platyhelminthes) that inhabit a variety of environments ranging from the intertidal zone to the deep sea. To date, only 17 polyclad species are recognized as mesopsammic (Smith et al. 2020; Tsuyuki et al. 2022, 2023a, 2023b, 2024), among which four belong to the genus *Boninia* Bock, 1923.

Boninia is the most species-rich genus in the family Boniniidae Bock, 1923, and is characterized by the presence of several prostatoid organs arranged in one or more girdles around the penis papilla and opening into the male antrum (Curini-Galletti and Campus 2007). Currently, this genus includes eight valid species: *Boninia antillarum* (Hyman 1955), *Boninia divae* Du Bois-Reymond Marcus & Marcus, 1968 (see Litvaitis et al. 2019 for potential synonymy with *B. antillarum*), *Boninia neotethydis* Curini-Galletti & Campus, 2007, *Boninia mirabilis* Bock, 1923, *Boninia oaxaquensis* Ramos-Sánchez, Bahia & Bastida-Zavala, 2020, *Boninia panamensis* Tsuyuki & Curini-Galletti, 2024, *Boninia uru* Tsuyuki, Oya & Kajihara,

Copyright *Liu, H.-L. et al.* This is an open access article distributed under the terms of the Creative Commons Attribution License (CC BY 4.0), which permits unrestricted use, distribution, and reproduction in any medium, provided the original author and source are credited.

2022, and *Boninia yambarensis* Tsuyuki, Oya & Kajihara, 2022. In addition, four undetermined species have been reported: *Boninia cf. uru* (Tsuyuki et al. 2024), *Boninia* sp. from the Philippines (Bock 1923; Curini-Galletti and Campus 2007), *Boninia* sp. from Costa Rica (Soutullo et al. 2021), and *Boninia* sp. from Panama (Laumer and Giribet 2014). The latter may correspond to *B. antillarum* (Tsuyuki et al. 2024). As noted by Tsuyuki et al. (2024), members of the genus *Boninia* share only a few diagnostic characters and are often superficially similar; therefore, molecular data are crucial for resolving their taxonomy.

In this study, we describe a new species of *Boninia* from the South China Sea by integrating morphological traits and DNA-based taxonomy. This represents the first record of boniniids from the coastal waters of China.

Materials and methods

Specimens were collected from intertidal coarse sand in Huidong, Guangdong Province, China, in April 2024. Live individuals were anesthetized using a 7.5% $MgCl_2$ solution prepared with tap water and were then photographed using a Leica MZ16 stereomicroscope (Leica Microsystems, Germany). A few anesthetized individuals were gently compressed with a coverslip and observed under a Nikon ECLIPSE Ni compound microscope (Nikon, Japan). The anterior part of each specimen was fixed in 95% EtOH for molecular analysis, whereas the posterior part was fixed in 10% formalin seawater for histological study. For histological examination, specimens were dehydrated through an ethanol series and cleared in xylene and were subsequently embedded in paraffin wax. Serial sections were cut at intervals of 7 µm and stained with modified Cason's Mallory–Heidenhain staining solution (Yang et al. 2020). Images were captured using a Nikon DS-Ri2 digital camera mounted on a Nikon ECLIPSE Ni compound microscope (Nikon, Japan). Histological preparations are deposited at the Marine Biological Museum, Chinese Academy of Sciences (MBMCAS), Qingdao, China.

Total DNA was extracted from ethanol-preserved specimens using the DNeasy Blood & Tissue Kit (QIAGEN), following the manufacturer's protocol. Fragments of the 18S rDNA (18S), 28S rDNA (28S), 16S rRNA (16S), and cytochrome c oxidase subunit I (COI) were amplified by polymerase chain reaction (PCR). Primers and PCR protocols are listed in the Suppl. material 1: table S1). The amplified products were sequenced at RuiBiotech (Guangzhou, China) using double-stranded Sanger sequencing to verify accuracy. Sequences were checked and edited using SeqMan software (DNAStar Inc.), and the final edited sequences were deposited in GenBank.

Phylogenetic analyses were performed using maximum likelihood (ML) and Bayesian inference (BI) methods with concatenated COI, 16S, 18S, and 28S sequences. A total of 22 terminal taxa were included in the phylogenetic analyses (Table 1). Sequences, except for COI, were aligned using MAFFT version 7 (Katoh and Standley 2013) with the "Auto" option. Ambiguous sites were removed using Gblocks version 0.91b (Castresana 2000) with a less stringent option. COI sequences were aligned and trimmed using MEGA 11 with ClustalW. TVM+G (16S), TVM+I+G (18S), TRN+I+G (28S), GTR+I (first codon positions of COI), TVM+I (second codon positions of COI), and TRN+I+G (third codon positions of COI) were selected as the optimal substitution models using PartitionFinder2 (Lanfear et

Table 1. List of species used for the molecular phylogenetic analysis.

Species	Locality	GenBank accession				Reference
		18S	28S	16S	COI	
B. antillarum 1	Tayrona National Park, Colombia	-	MH700279	-	-	Litvaitis et al. (2019)
B. antillarum 2	Playa Santa Ceuz, Curaçao	-	MH700280	-	-	Litvaitis et al. (2019)
B. antillarum 3	Jamaica	-	MH700281	-	-	Litvaitis et al. (2019)
B. antillarum 4	Great Lameshure Bay, St. John, US Virgin Islands	-	MH700282	-	-	Litvaitis et al. (2019)
B. neotethydis	Eilat, Israel	-	MH700283	-	-	Litvaitis et al. (2019)
B. oaxaquensis 1	Achotines, Panama		LC795616		LC795625	Tsuyuki et al. (2024)
B. oaxaquensis 2	Achotines, Panama	LC795612	LC795617	LC795623	LC795626	Tsuyuki et al. (2024)
B. oaxaquensis 3	Playa Langosta, Costa Rica	MZ292819	MZ292834	MZ292869	-	Cuadrado et al. (2024)
B. panamensis 1	Achotines, Panama	LC795613	LC795618	LC795624	LC795627	Tsuyuki et al. (2024)
B. panamensis 2	Naos, Panama	LC795614	LC795619	-	-	Tsuyuki et al. (2024)
B. panamensis 3	Naos, Panama				LC795628	Tsuyuki et al. (2024)
B. cf. uru 1	Hilo, Hawai'i, USA	-	LC795622	-	LC795629	Tsuyuki et al. (2024)
B. cf. uru 2	O'ahu, Hawai'i, USA		LC795621			Tsuyuki et al. (2024)
B. cf. uru 3	O'ahu, Hawai'i, USA	LC795615	LC795620	-	LC795630	Tsuyuki et al. (2024)
B. uru	Okinawa Island, Japan	LC699274	LC699276	-	LC699269	Tsuyuki et al. (2022)
B. yambarensis	Okinawa Island, Japan	LC699273	LC699278	-	LC699272	Tsuyuki et al. (2022)
B. divae	Bocas del Toro, Panama	KC869793	KC869846	KC869751	-	Laumer and Giribet (2014)
B. corolla sp. nov.	Huidong, China	PX511556	PX511559	PX511553	PX511324	This study
Outgroup						
P. flavomarginata	Kagoshima, Japan	LC672041	LC568535		LC568538	Tsuyuki et al. (2020)
P. tectivorum	Aquaria Innsbruck, Austria	MN334202	MK181524		-	Dittmann et al. (2019)
T. mediterranea	Rovinj, Croatia	MN384707	MN384705		-	Dittmann et al. (2019)
Theama sp.	Bocas del Toro, Panama	KC869792	KC869845		-	Litvaitis et al. (2019)

al. 2016) under the corrected Akaike Information Criterion (AICc) with the greedy algorithm. Maximum likelihood analyses were conducted using IQ-TREE 2 (Minh et al. 2020) with the edge-linked partition model (Chernomor et al. 2016). Bayesian inference (BI) was performed using MrBayes version 3.2.2 (Ronquist et al. 2012). MrBayes was run for 3 million generations, sampling one tree every 1000 generations, with two parallel runs and four independent Markov chains per run. The standard deviation of split frequencies (< 0.01) was used as the criterion to assess convergence.

Two species delimitation analyses, Bayesian Poisson Tree Processes (bPTP) (Zhang et al. 2013) and Automatic Barcode Gap Discovery (ABGD) (Puillandre et al. 2012), were conducted. For the bPTP analysis, a ML tree generated from the concatenated datasets was used as input and analyzed on the web server (http://species.h-its.org/ptp/) with the following parameters: MCMC, 100000 generations; thinning, 100; burn-in, 0.1; seed, 123. Convergence was always checked. The ABGD analysis was performed on the iTaxoTools Galaxy Server (Vences et al. 2021) using the COI marker with the following settings: Pmin, 0.001; Pmax, 0.1; steps, 10; X (relative gap width), 1.0; number of bins for distance distribution, 20; and distance, Kimura two-parameter (K80) TS/TV 2.0. Uncorrected p-distances for COI, 16S, and 28S were calculated in MEGA version 10 (Kumar et al. 2018).

Results

Family Boniniidae Bock, 1923
Genus *Boninia* Bock, 1923

***Boninia corolla* Liu & He, sp. nov.**
https://zoobank.org/AA858F28-766A-4587-892C-9964A0BD53FF

Etymology. The species name *corolla* is a Latin noun meaning "flower crown", referring to the radially arranged prostatoid organs around the male atrium that look like a flower.

Material examined. ***Holotype*:** • MBM288498, Da'ao Village Beach (22°33.50'N, 114°53.33'E), Huidong, Guangdong Province, China; coarse-grained sand, 28 April 2024, coll. Hai-Long Liu; sagittal sections on five slides, deposited at MBMCAS; GenBank accession: PX511324 (COI), PX511553 (16S), PX511556 (18S), and PX511559 (28S). ***Paratypes*:** • MBM288499, sagittal sections on 4 slides, same data as for holotype; GenBank accession: PX511554 (16S), PX511557 (18S), and PX511560 (28S). MBM288500, sagittal sections on four slides, same data as for holotype; GenBank accession: PX511555 (16S), PX511558 (18S), and PX511561 (28S).

Description. The worm is flat and slender, translucent milky-white, and with tapering posterior end (Fig. 1A). Anesthetized specimens are 14–26 mm long and 0.8–1.2 mm wide. A pair of fine, flexible tentacles (approximately 0.5 mm long) is present on either side of head (Fig. 1B).

The tentacular eyes are absent. A pair of cerebral eyespots is symmetrically located at the anterior margin of the brain, with the two eyespots in each pair lying closely together (Fig. 1B). Marginal eyespots, 28–48 in number, are evenly distributed along the base of the tentacles, extending to the posterior margin of the brain (Fig. 1B).

The intestine is highly branched and darkened by gut contents. A ruffled pharynx is 7–11 mm long and is located at or slightly posterior to the center of the body (Fig. 1A). The mouth opens slightly anterior to the center of the pharynx. The male pore lies approximately 1 mm behind the posterior end of the pharynx (Fig. 1D). The female pore opens 1.5–2.0 mm posterior to the male pore (Figs 1D, 2F). An adhesive organ is located at the posterior end of body on ventral side.

The male copulatory apparatus is comprised of a seminal vesicle, an interpolated prostatoid, a penis papilla, and 9–15 prostatoid organs. A pair of sperm ducts extends along each side of the midline, curves at the posterior region of the pharynx, and enters the seminal vesicle separately (Fig. 1D). The seminal vesicle is somewhat ovoid (Fig. 2A, F), with both ends elongated, and the distal end opening into the prostatic vesicle (Fig. 2A, F). The seminal vesicle is lined with a flat, ciliated epithelium and surrounded by a layer of very strong circular muscle fibers, especially near the distal part; a few longitudinal muscle layers lie external to the circular fibers (Fig. 2A, F). The prostatic vesicle is nearly heart-shaped (50 μm in its long axis, 25 μm in its short axis), lined with high epithelium, and connects to penis papilla (Fig. 2A, F). The penis papilla is unarmed and projects into the male atrium (Fig. 2A, F). The inner wall of the male atrium is ciliated. The individual ducts of 9–15 prostatoid organs are radially arranged into a single girdle around the male atrium (Figs 1C, 2C) and open into inner area of the male atrium (Fig. 2A, F). Each pyriform prostatoid organ bears a sclerotized stylet (approximately 60 μm in length) (Figs 1C, 2D). Extracapsular glands produce glandular secretion into each prostatoid organ (Fig. 2C, D, F).

The ovaries are dorsally arranged in two rows, one on each side of the body, extending from behind the brain to almost the posterior end of the body. A pair of uterine canals, posterior to the male copulatory organ, are connected through short lateral branches to multiple uterine vesicles (approximately 10–17 in number on each side) (Fig. 1D, E). Each uterine canal widens distally to form a large posterior dilation filled with eggs (Fig. 1D, E). The uterine canals connect to the vagina immediately anterior to the entrance of Lang's vesicle (Figs 1D, 2B, E, F). The Lang's vesicle is elongated (240 μm in its long axis; 150 μm in its short axis) and is lined with ciliated epithelium (Fig. 2B, E). The ciliated vagina extends anteriorly for a short distance, then turns ventrally to dilate and form a shell chamber, which is surrounded by numerous cement glands (Fig. 2B, E). The vagina continues its course to open externally through the female genital pore.

Distribution. The species is known from the type locality, Huidong, Guangdong, China.

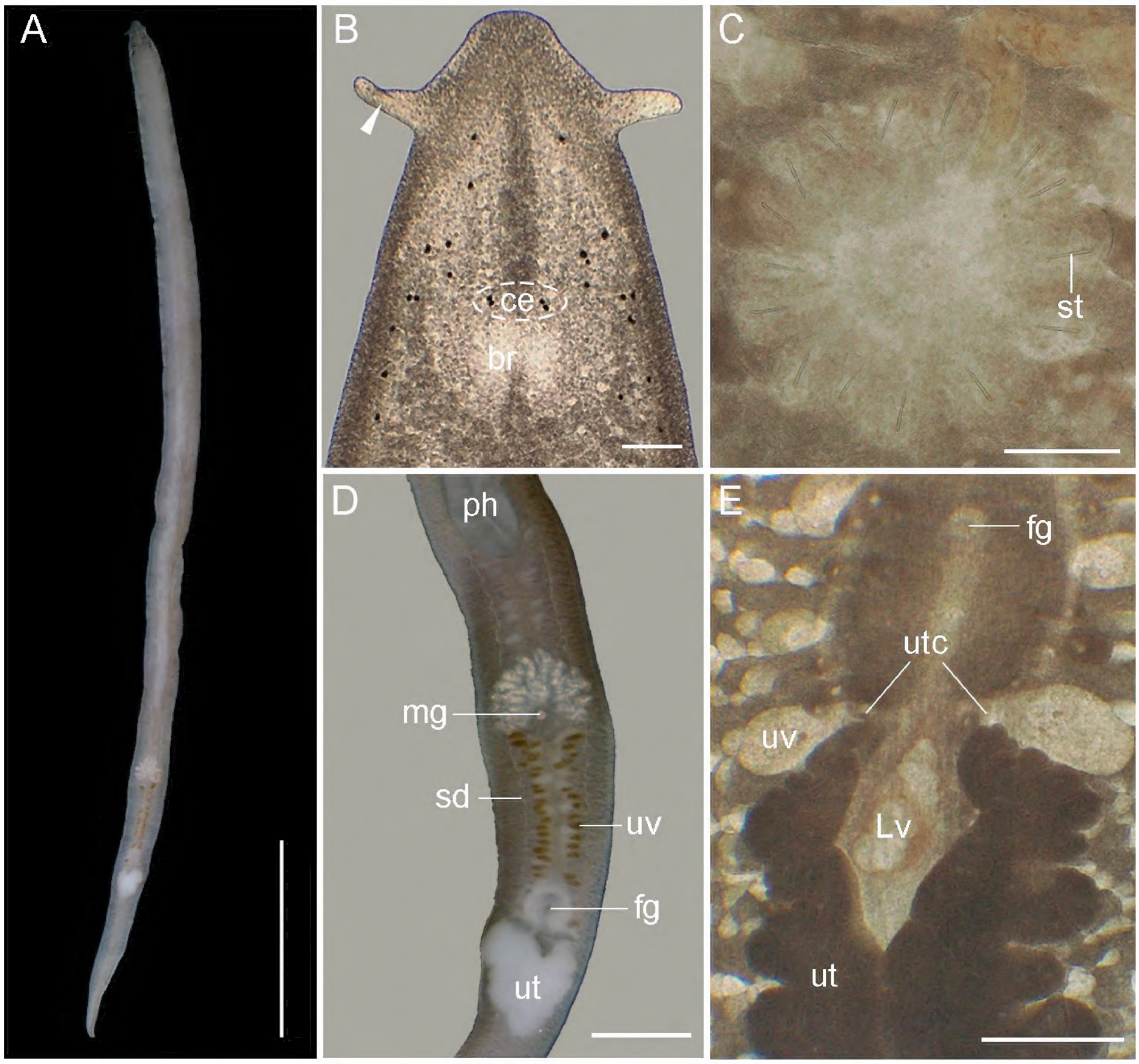

Figure 1. *Boninia corolla* sp. nov. **A.** Photograph of entire body; **B.** Magnification of head (squeezed); **C.** Arrangement of prostatoid organs (squeezed); **D.** Copulatory complex (squeezed); **E.** Photograph of the female copulatory organ (squeezed). Pointed tentacles are shown by the arrowhead (**B**). Abbreviations: br – brain; ce – cerebral eyes; fg – female gonopore; Lv – Lang's vesicle; mg – male gonopore; sd – sperm duct; st – stylet; ut – uterine; utc – uterine canal; uv – uterine vesicle. Scale bars: 5 mm (**A**); 100 µm (**B**); 50 µm (**C**); 1 mm (**D**); 200 µm (**E**).

Habitat. Intertidal, coarse-grained sand.

Molecular phylogeny, DNA taxonomy, and genetic distances. Our BI and ML trees are almost identical to each other in topology. All *Boninia* species form a clade with high support values (BP = 100%, PP = 1) (Fig. 3). *Boninia corolla* sp. nov. is sister to a clade composed of all other species of the genus except *B. yambarensis* and *B. neotethydis*, with support values (BP = 72%, PP = 0.96). For species delimitation, the bPTP analysis results in 8 entities for the concatenated dataset, and ABGD results in 6 entities for COI (Fig. 3, Suppl. material 1: fig. S1). Notably, both delimitation approaches consistently supported *Boninia corolla* sp. nov. as a distinct species (Fig. 3). The uncorrected p-distances for the COI, 16S, and 28S in *Boninia* are shown in Tables 2–4, respectively. Intraspecific genetic distances ranged from 0.00–0.42% for COI, 0.24–0.47% for 16S, and 0.00–0.13% for 28S. Interspecific genetic distances ranged from 10.72–22.14% for COI, 2.58–21.02% for 16S, and 0.50–4.01% for 28S, with the exception of *B. uru* and *B. cf. uru*, which showed no divergence, 0.00%.

Discussion

Our specimens are assigned to the genus *Boninia* based on the following characters: (i) a narrow and elongated body with two pointed tentacles on the anterolateral margins of the head; (ii) 9–15 prostatoid organs with stylets arranged into a single girdle; (iii) the presence of Lang's

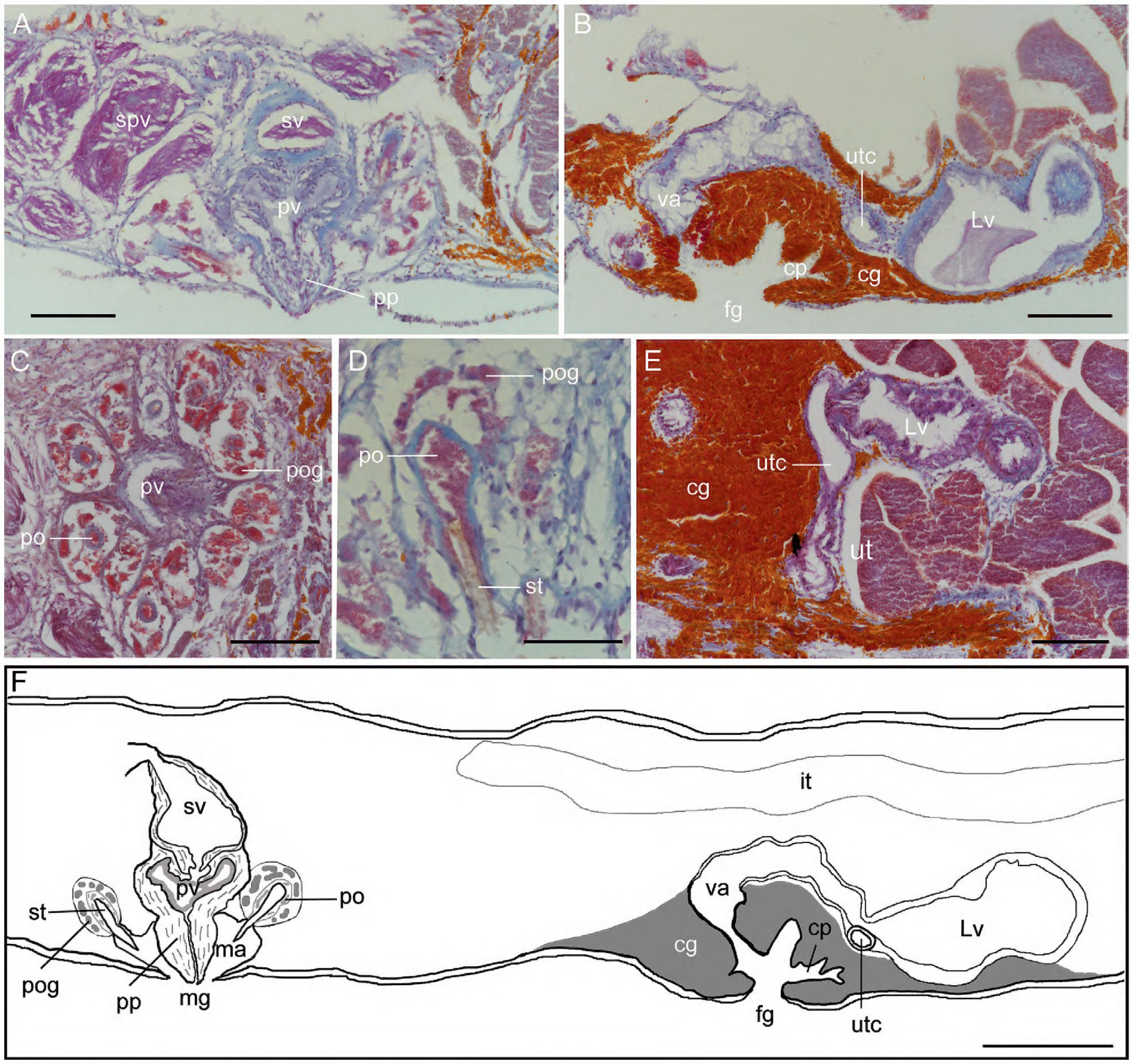

Figure 2. *Boninia corolla* sp. nov., MBM288498 (holotype), photomicrographs of sagittal sections (**A, B, D**); MBM288499 (paratype), photomicrographs of cross sections (**C, E**); schematic diagram (**F**). **A.** Male copulatory organ; **B, E.** Female copulatory organ; **C.** Arrangement of prostatoid organs; **D.** Prostatoid organ; **F.** Copulatory complex. Abbreviations: cg – cement glands; cp – cement pouch; fg – female gonopore; it – intestine; Lv – Lang's vesicle; ma – male atrium; mg – male gonopore; po – prostatoid organ; pog – prostatoid organ glands; pp – penis papilla; pv – prostatoid vesicle; spv – sperm vesicle; st – stylet; sv – seminal vesicle; ut – uterine; utc – uterine canal; va – vagina. Scale bars: 100 µm (**A, B, C, E**); 50 µm (**D**); 200 µm (**F**).

Table 2. Uncorrected p-distances (%) of the COI gene fragments (705 bp) among selected *Boninia* species.

	B. oaxaquensis	***B. panamensis***	***B. cf. uru***	***B. uru***	***B. yambarensis***	***B. corolla* sp. nov.**
B. oaxaquensis (n = 2)	0.00					
B. panamensis (n = 2)	20.45	0.00				
B. cf. uru (n = 2)	21.30–21.44	16.93–17.35	0.42			
B. uru	20.73	15.8	10.72–11.14	-		
B. yambarensis	22.14	18.76	21.30–21.44	20.45	-	
B. corolla sp. nov.	20.87	20.31	20.03	19.18	19.32	-

vesicle; and (iv) a ventral adhesive organ located at the posterior end of the body. Currently, this genus includes eight named species: *B. antillarum*, *B. divae*, *B. neotethydis*, *B. mirabilis*, *B. oaxaquensis*, *B. panamensis*, *B. uru*, and *B. yambarensis*. Among them, *Boninia corolla* sp. nov. is easily distinguishable from *B. antillarum*, *B. divae*, and *B. mirabilis* by its single girdle of prostatoid organs (Bock 1923; Curini-Galletti and Campus 2007) (Table 5). The remaining five species of the genus also possess a single girdle of prostatoid organs;

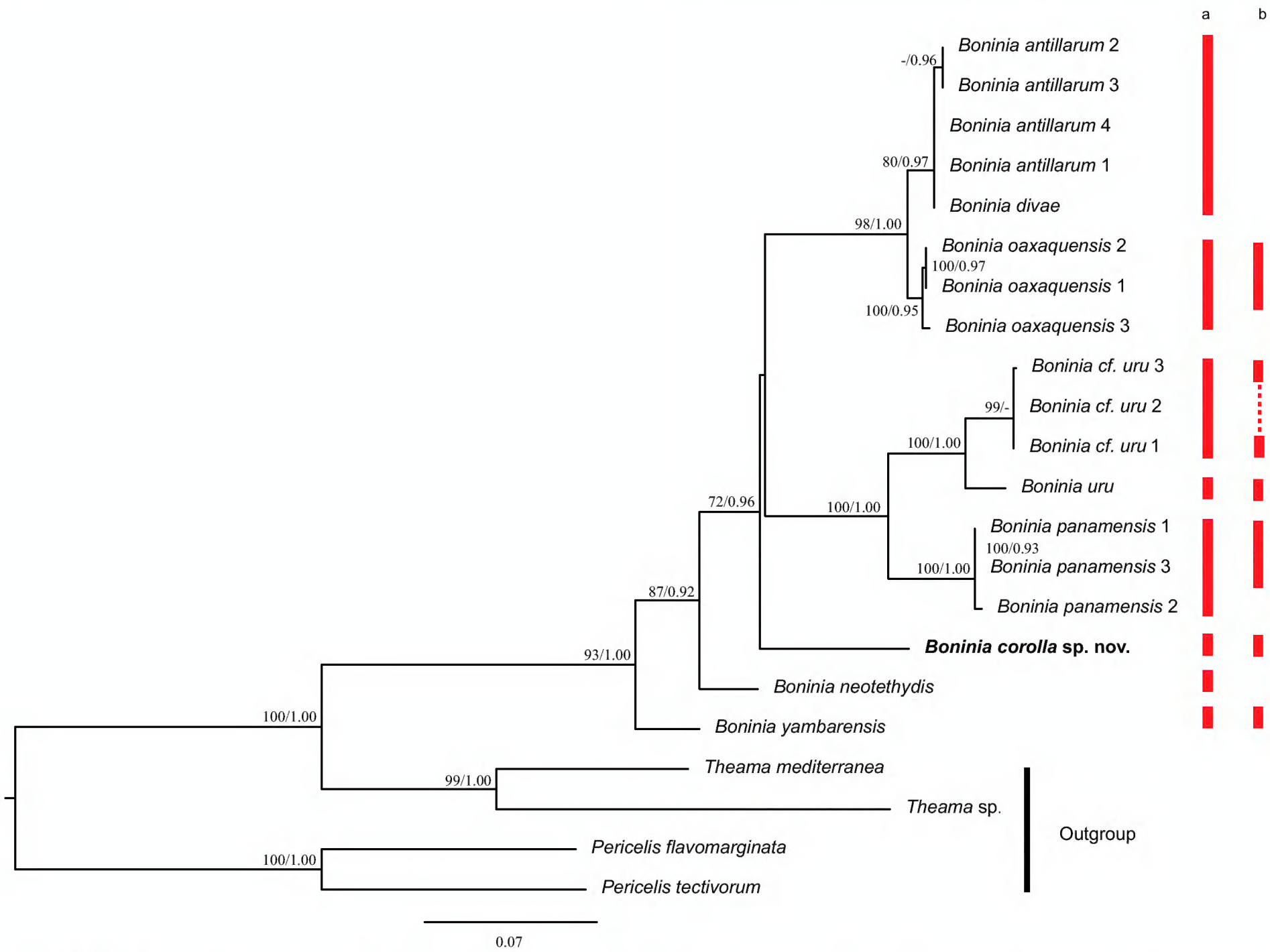

Figure 3. Phylogenetic tree and results of species delimitation analyses. Maximum likelihood phylogenetic tree based on the concatenated dataset (COI, 16S, 18S, and 28S). Bootstrap support values > 70 and Bayesian posterior probabilities > 0.90 are provided as numbers next to nodes. Results of bPTP and ABGD analyses are indicated by red vertical bars (a, bPTP for the concatenated dataset; b, ABGD for COI).

Table 3. Uncorrected p-distances (%) of the 16S gene fragments (427 bp) among selected *Boninia* species.

	***B. corolla* sp. nov.**	***B. oaxaquensis***	***B. divae***	***B. panamensis***
B. corolla sp. nov. (n = 3)	0.24–0.47			
B. oaxaquensis (n = 2)	13.92–14.50	0.30		
B. divae	14.35–14.62	2.58–3.00	-	
B. panamensis	18.20–14.72	19.58–21.02	19.76	-

Table 4. Uncorrected p-distances (%) of the 28S gene fragments (948 bp) among selected *Boninia* species.

	B. antillarum	***B. divae***	***B. oaxaquensis***	***B. yambarensis***	***B. neotethydis***	***B. corolla* sp. nov.**	***B. panamensis***	***B. cf. uru***	***B. uru***
B. antillarum (n = 4)	0.00–0.11								
B. divae	0.11	-							
B. oaxaquensis (n = 3)	0.50–0.63	0.50–0.53	0.13						
B. yambarensis	1.58–1.69	1.69	1.37–1.63	-					
B. neotethydis	1.48–1.69	1.69	1.50–1.58	1.48	-				
B. corolla sp. nov. (n = 3)	2.43–2.64	2.64	2.74–2.88	2.43	2.64	0.00			
B. panamensis (n = 2)	2.96–3.18	2.96–3.06	1.50–2.75	3.06–3.17	2.85–2.96	3.91–4.01	0.11–0.11		
B. cf. uru (n = 3)	2.96–3.07	2.96	2.85–3.00	3.06	3.06	3.70	1.06–1.16	0.00	
B. uru	2.96–3.07	2.96	2.85–3.00	3.06	3.06	3.70	1.06–1.16	0.00	-

however, the new species is distinguishable from *B. uru*, *B. cf. uru*, *B. panamensis*, *B. oaxaquensis*, and *B. yambarensis* by the number of prostatoid organs (9–15 in *B. corolla* sp. nov., compared with 2–4 in *B. uru*, 2 in *B. cf. uru* and *B. panamensis*, 16–24 in *B. oaxaquensis*, and 21–22 in *B. yambarensis*) (Ramos-Sánchez et al. 2020; Tsuyuki et al. 2022; Tsuyuki et al. 2024) (Table 5). In addition, *B. corolla* sp. nov. differs from *B. neotethydis* in body size (14–26 mm long and approximately 1 mm wide in *B. corolla* sp. nov. versus 60 mm long

Table 5. Comparison of characters among *Boninia* species.

Species	*B. corolla* sp. nov.	*B. antillarum*	*B. divae*	*B. mirabilis*	*B. neotethydis*
Body size	14–26 mm (L), 0.8–1.2 mm (W)	8 mm (L), 2 mm (W); 16 mm (L), 3.3–3.9 mm (W)	30–50 mm (L), 2–4 mm (W)	29 mm (L), 4.5 mm (W) (preserved state)	60 mm (L), 5 mm (W)
Marginal eyespot number	28–48, only dorsally	about 40	numerous	numerous, present dorsally and ventrally	10–18 (3–8 per side)
Cerebral eyespot number	4	about 30	numerous	13	4
Pharynx length	7–11 mm	4.5–5 mm	12.5 mm	?	?
Prostatoid organ number	9–15	25; < 30	> 50	about 40	10–18
Girdle	single	triple	triple	double	single
Uterine vesicle number	10–17 in each	several	8–10 in each	5 in each	several
Inner wall of Lang's vesicle	ciliated	nonciliated	ciliated	ciliated	partly ciliated
Connection point of uterine canals	vagina immediately anterior to the entrance of Lang's vesicle	vagina immediately anterior to the entrance of Lang's vesicle	vagina immediately anterior to the entrance of Lang's vesicle	vagina immediately anterior to the entrance of Lang's vesicle	a diverticulum of the vaginal duct close to Lang's vesicle
Habitat	coarse sediments	under stones at high waterline; beach rock	under stones at high water lined	under stones near the high-water limit	coarse sediments
Reference	this study	Hyman 1955; Du Bois-Reymond Marcus and Marcus 1968; Curini-Galletti and Campus 2007	Hyman 1955; Du Bois-Reymond Marcus and Marcus 1968	Bock 1923; Curini-Galletti and Campus 2007	Curini-Galletti and Campus 2007
Species	***B. oaxaquensis***	***B. uru***	***B. cf. uru***	***B. yambarensis***	***B. panamensis***
Body size	3–11 mm (L), 1–3 mm (W)	3–4.5 mm (L), 0.65–0.9 mm (W)	5–6 mm (L)	13.9–22.4 mm (L), 0.93–1.25 mm (W)	5–8 mm (L), 1.7 mm (W)
Marginal eyespot number	36–126	21–29, only dorsally	25–34; present dorsally and ventrally	19–42, only dorsally	61–80
Cerebral eyespot number	14–66	4	4	6–7	4
Pharynx length	1.2 mm	0.5–1.1 mm	0.34–0.6 mm	2.6–6.6 mm	1.5 mm
Prostatoid organ number	16–24	2–4	2	21–22	2
Girdle	single	single	single	single	single
Uterine vesicle number	?	2 in each	3–4 in each	5 in each	2 in each
Inner wall of Lang's vesicle	?	lined with cilia; elongated in posterior region	lined with longer cilia	lined with cilia; elongated in posterior region	ciliated in its antero-ventral part
Connection point of uterine canals	?	lateral to Lang's vesicle	lateral to Lang's vesicle	vagina immediately anterior to the entrance of Lang's vesicle	lateral to Lang's vesicle
Habitat	under littoral to sublittoral rocks	interstitial coarse sand	interstitial coarse sand	under intertidal rocks	interstitial coarse sand
Reference	Ramos-Sánchez et al. 2020; Tsuyuki et al. 2024	Tsuyuki et al. 2022	Tsuyuki et al. 2022	Tsuyuki et al. 2022	Tsuyuki et al. 2022

and 5 mm wide in *B. neotethydis*) and in the number of marginal eyespots (28–48 in *B. corolla* sp. nov. versus 10–18 in *B. neotethydis*). Furthermore, in *B. neotethydis*, the uterine canals enter a diverticulum of the vaginal duct close to Lang's vesicle (see Curini-Galletti and Campus 2007: fig. 3B), whereas in *B. corolla* sp. nov., this diverticulum is absent, and the uterine canals connect to the vagina immediately anterior to the entrance of Lang's vesicle. The taxonomic relevance of the position of the uterine canal connections, whether lateral to Lang's vesicle or immediately anterior to it, has been emphasized in studies of the genus *Boninia*. However, histological sections are not available for all species, and some reconstructions rely solely on observations of squeezed living specimens. Notably, these positions are spatially very close to one another, and given this proximity, the taxonomic significance of this difference may have been overestimated. By contrast, *B. neotethydis* is distinct, as its uterine canals enter a diverticulum of the vaginal duct close to Lang's vesicle, whereas this feature is absent in other *Boninia* species for which histological sections are available. Therefore, we suggest that the position of the uterine canal connections should be interpreted with caution until additional histological material becomes available for more species of the genus.

Our phylogenetic results are consistent with those of Tsuyuki et al. (2024), in that all *Boninia* species formed a well-supported clade. *Boninia corolla* sp. nov. is nested within the *Boninia* clade, which corroborates its generic assignment based on morphology. Both bPTP and ABGD analyses further supported *Boninia corolla* sp. nov. as a distinct species.

The ranges of intra- and interspecific genetic distances for COI and 16S did not overlap; interspecific divergence was more than 20-fold greater than intraspecific variation for COI and more than 10-fold greater for 16S. These results indicate that COI and 16S are effective markers for DNA barcoding for *Boninia* species in this study. Although the ranges of intra- and interspecific genetic distances for 28S showed no divergence between *B. uru* and *B. cf. uru*, the remaining species could still be distinguished using

this marker. Genetic distances between *B. corolla* sp. nov. and other examined species ranged from 19.18 to 20.87% for COI, 13.92 to 18.72% for 16S, and 2.43 to 2.74% for 28S, all of which exceed the smallest interspecific distances observed among *Boninia* species and therefore support the establishment of *B. corolla* as a new species.

Acknowledgments

This study was supported by grants from the Scientific and Technical Innovation Council of the Shenzhen Government (No. JCYJ20210324093412035) and the Special Program of Key Sectors in Guangdong Universities (No. 2022ZDZX4040).

References

Bock S (1923) *Boninia*, a new polyclad genus from the Pacific. Nova Acta Regiae Societatis Scientiarum Upsaliensis 6(4): 1–32.

Castresana J (2000) Selection of conserved blocks from multiple alignments for their use in phylogenetic analysis. Molecular Biology and Evolution 17(4): 540–552. https://doi.org/10.1093/oxfordjournals.molbev.a026334

Cerca J, Purschke G, Struck TH (2018) Marine connectivity dynamics: Clarifying cosmopolitan distributions of marine interstitial invertebrates and the meiofauna paradox. Marine Biology 165: 123. https://doi.org/10.1007/s00227-018-3383-2

Chernomor O, von Haeseler A, Minh BQ (2016) Terrace aware data structure for phylogenomic inference from supermatrices. Systematic Biology 65(6): 997–1008. https://doi.org/10.1093/sysbio/syw037

Cuadrado D, Rodríguez J, Machordom A, Noreña C, Fernández-Álvarez FÁ, Hutchings P, Williamson J (2024) Base-substitution rates of nuclear and mitochondrial genes for polyclad flatworms. Zoosystematics and Evolution 100: 863–876. https://doi.org/10.3897/zse.100.119945

Curini-Galletti M, Campus P (2007) *Boninia neotethydis* sp. nov. (Platyhelminthes: Polycladida: Cotylea)—the first lessepsian flatworm. The European Zoological Journal 87: 435–442. https://doi.org/10.1017/S0025315407055014

Dittmann IL, Cuadrado D, Aguado MT, Noreña C, Egger B (2019) Polyclad phylogeny persists to be problematic. Organisms, Diversity & Evolution 19: 585–608. https://doi.org/10.1007/s13127-019-00415-1

Du Bois-Reymond Marcus E, Marcus E (1968) Polycladida from Curaçao and faunistically related regions. Studies on the fauna of Curaçao and other Caribbean Islands 101: 1–133.

Higgins RP, Thiel H (1988) Introduction to the Study of Meiofauna. Smithsonian Institution Press, Washington, DC.

Hyman LH (1955) Some polyclad flatworms from the West Indies and Florida. Proceedings of the United States National Museum 104: 115–150. https://doi.org/10.5479/si.00963801.104-3341.115

Katoh K, Standley DM (2013) MAFFT multiple sequence alignment software version 7: Improvements in performance and usability. Molecular Biology and Evolution 30(4): 772–780. https://doi.org/10.1093/molbev/mst010

Kumar S, Stecher G, Li M, Knyaz C, Tamura K (2018) MEGA X: Molecular evolutionary genetics analysis across computing platforms. Molecular Biology and Evolution 35(6): 1547–1549. https://doi.org/10.1093/molbev/msy096

Lanfear R, Frandsen PB, Wright AM, Senfeld T, Calcott B (2016) PartitionFinder 2: New methods for selecting partitioned models of evolution for molecular and morphological phylogenetic analyses. Molecular Biology and Evolution 34: 772–773. https://doi.org/10.1093/molbev/msw260

Laumer CE, Giribet G (2014) Inclusive taxon sampling suggests a single, stepwise origin of ectolecithality in Platyhelminthes. Biological Journal of the Linnean Society. Linnean Society of London 111: 570–588. https://doi.org/10.1111/bij.12236

Litvaitis MK, Bolaños DM, Quiroga SY (2019) Systematic congruence in Polycladida (Platyhelminthes, Rhabditophora): Are DNA and morphology telling the same story? Zoological Journal of the Linnean Society 186: 865–891. https://doi.org/10.1093/zoolinnean/zlz007

Liu HL, Kajihara H, Sun SC (2022) Diversity of interstitial nemerteans of the genus *Ototyphlonemertes* (Nemertea: Monostilifera: Ototyphlonemertidae) in the South China Sea, with a comment on the distribution pattern of the genus. Frontiers in Marine Science 9: 1009536. https://doi.org/10.3389/fmars.2022.1009536

Minh BQ, Schmidt HA, Chernomor O, Schrempf D, Woodhams MD, von Haeseler A, Lanfear R (2020) IQ-TREE 2: New models and efficient methods for phylogenetic inference in the genomic era. Molecular Biology and Evolution 37: 1530–1534. https://doi.org/10.1093/molbev/msaa015

Puillandre N, Lambert A, Brouillet S, Achaz G (2012) ABGD, automatic barcode gap discovery for primary species delimitation. Molecular Ecology 21: 1864–1877. https://doi.org/10.1111/j.1365-294X.2011.05239.x

Ramos-Sánchez M, Bahia J, Bastida-Zavala JR (2020) Five new species of cotylean flatworms (Platyhelminthes: Polycladida: Cotylea) from Oaxaca, southern Mexican Pacific. Zootaxa 4819: 49–83. https://doi.org/10.11646/zootaxa.4819.1.3

Ronquist F, Teslenko M, van der Mark P, Ayres DL, Darling A, Höhna S, Larget B, Liu L, Suchard MA, Huelsenbeck JP (2012) MrBayes 3.2: Efficient Bayesian phylogenetic inference and model choice across a large model space. Systematic Biology 61(3): 539–542. https://doi.org/10.1093/sysbio/sys029

Smith JPS III, Steenkiste NV, Artois T (2020) Platyhelminthes. In: Schmidt-Rhaesa A (Ed.) Guide to the Identification of Marine Meiofauna. Verlag Dr. Friedrich Pfeil, Munich, Germany, 54–103.

Soutullo P, Cuadrado D, Noreña C (2021) First study of the Polycladida (Rhabditophora, Platyhelminthes) from the Pacific Coast of Costa Rica. Zootaxa 4964: 363–381. https://doi.org/10.11646/zootaxa.4964.2.7

Swedmark B (1964) The interstitial fauna of marine sand. Biological Reviews of the Cambridge Philosophical Society 39: 1–42. https://doi.org/10.1111/j.1469-185X.1964.tb00948.x

Tsuyuki A, Oya Y, Jimi N, Kajihara H (2020) Description of *Pericelis flavomarginata* sp. nov. (Polycladida: Cotylea) and its predatory behavior on a scaleworm. Zootaxa 4894: 403–412. https://doi.org/10.11646/zootaxa.4894.3.6

Tsuyuki A, Oya Y, Kajihara H (2022) Reversible shifts between interstitial and epibenthic habitats in evolutionary history: molecular phylogeny of the marine flatworm family Boniniidae (Platyhelminthes:

Polycladida: Cotylea) with descriptions of two new species. PLoS ONE 17: e0276847. https://doi.org/10.1371/journal.pone.0276847

Tsuyuki A, Oya Y, Jimi N, Hookabe N, Fujimoto S, Kajihara H (2023a) *Theama japonica* sp. nov., an interstitial polyclad flatworm showing a wide distribution along Japanese Coasts. Zoological Science 40: 262–272. https://doi.org/10.2108/zs220105

Tsuyuki A, Oya Y, Kajihara H (2023b) A new species of slender flatworm in the genus *Eucestoplana* and a record of *E.* cf. *cuneata* (Platyhelminthes, Polycladida) from the Okinawa Islands, Japan, with an inference of their phylogenetic positions within Cestoplanidae. Zoosystematics and Evolution 99: 363–373. https://doi.org/10.3897/zse.99.102604

Tsuyuki A, Norenburg J, Leasi F, Curini-Galletti M (2024) Molecular phylogeny of *Boninia* (Platyhelminthes: Polycladida), with description of a new species from the Pacific coasts of Panama. Invertebrate Systematics 38: IS24009. https://doi.org/10.1071/IS24009

Vences M, Miralles A, Brouillet S, Ducasse J, Fedosov A, Kharchev V, Kostadinov I, Kumari S, Patmanidis S, Scherz MD, Puillandre N, Renner SS (2021) iTaxoTools 0.1: Kickstarting a specimen-based software toolkit for taxonomists. Megataxa 6(2): 77–92. https://doi.org/10.11646/megataxa.6.2.1

Worsaae K, Kristensen RM (2005) Evolution of interstital Polychaeta (Annelida). Hydrobiologia 535–536: 319–340. https://doi.org/10.1007/s10750-004-4417-y

Yang Y, Li JY, Sluys R, Li WX, Li SF, Wang AT (2020) Unique mating behavior, and reproductive biology of a simultaneous hermaphroditic marine flatworm (Platyhelminthes, Tricladida, Maricola). Invertebrate Biology 139(1): e12282. https://doi.org/10.1111/ivb.12282

Zhang J, Kapli P, Pavlidis P, Stamatakis A (2013) A general species delimitation method with applications to phylogenetic placements. Bioinformatics 29: 2869–2876. https://doi.org/10.1093/bioinformatics/btt499

Supplementary material 1

Supplementary information

Authors: Hai-Long Liu, Bing-Bing He, An-Tai Wang, Shuang-Fei Li, Yu Zhang

Data type: doc

Explanation note: **table S1.** List of primers used in this study. **figure S1.** PTP species delimitation result on concatenated data set.

Copyright notice: This dataset is made available under the Open Database License (http://opendatacommons.org/licenses/odbl/1.0/). The Open Database License (ODbL) is a license agreement intended to allow users to freely share, modify, and use this Dataset while maintaining this same freedom for others, provided that the original source and author(s) are credited.

Link: https://doi.org/10.3897/zse.102.175615.suppl1